Experimental Investigations of the Influence of Molecular Weight Distribution on Melt Spinning and Extrudate Swell Characteristics of Polypropylene

WATARU MINOSHIMA, JAMES L. WHITE, and JOSEPH E. SPRUIELL,
Polymer Engineering, The University of Tennessee, Knoxville, Tennessee 37916

Synopsis

An experimental study of the influence of molecular weight distribution on the melt spinning and extrudate swell of a series of polypropylenes of varying molecular weight and distribution is reported. Emphasis is given to effects of variations of molecular weight distribution. Narrowing the molecular distribution increases the slope of the elongational viscosity–elongation rate curve, stabilizes the spinline relative to both random disturbances and draw resonance, and decreases both instantaneous and delayed extrudate swell. These results are interpreted in terms of viscoelastic fluid mechanics and earlier experimental studies by the authors of the influence of molecular weight distribution on rheological properties. The influences of these rheological factors on spinline structure development is discussed.

INTRODUCTION

Polypropylene is becoming of increased importance as a plastic and fiber because of its economics and the range of mechanical and performance characteristics which may be attained through processing. As with most polymers it is possible to produce polypropylenes of varying molecular weight and distribution. It is thus of considerable interest to study the relative processing characteristics of polymer melts exhibiting such a range of structures. In this paper we make a basic study of the problems of melt spinning and extrudate swell with polypropylenes of varying molecular weight and distribution. We seek also to interpret these processing characteristics in terms of theoretical analyses of viscoelastic fluid mechanics.

We first study the melt spinning characteristics under isothermal conditions, specifically the apparent spinline elongational viscosity χ_{sp} as a function of elongation rate in the spinline. Studies of the apparent isothermal spinline elongational viscosity of individual polymer melts have been reported by Acierno, Dalton, Rodriquez, and White,[1] Han, Lamonte, and Kim,[2] Bankar, Spruiell, and White,[3] and Hill and Cuculo,[4] among others. The polymers investigated include low-density polyethylene (LDPE),[1,2] high-density polyethylene (HDPE),[2] polystyrene (PS),[1,2] polypropylene (PP),[2] nylon 6,[3] and poly(ethylene terephthalate).[4] No organized study showing the influence of molecular weight and its distribution has been reported. We report such a study for polypropylene here.

We also investigate spinline instabilities. The failure of polypropylene fibers

Journal of Applied Polymer Science, Vol. 25, 287–306 (1980)

0021-8995/80/0025-0287$01.00

during melt spinning has been studied as a function of molecular weight by Ishizuka, Murase, Koyama, and Aoki.[5] Fibers produced by melt spinning frequently exhibit spinline diameter fluctuations. This has been observed in a wide range of polymers but notably in polypropylene.[6–13] Similar thickness fluctuations are observed in extruded ribbon, cast film, and extrusion coating operations.[9,11,14–16] These phenomena are often collectively called "draw resonance," though different initiation mechanisms may exist. High-density polyethylene also exhibits a strong draw resonance behavior, while the effect is greatly reduced in PS and apparently almost nonexistent in LDPE. Bergonzoni and DiCresci[15] investigated the influence of molecular weight on the occurrence of draw resonance and found it to become increasingly severe with increase of molecular weight. However, these authors did not investigate variations in molecular weight distribution. We take this into account in the present paper.

We also present a study of extrudate swell of polypropylene melts emerging from single-hole spinnerets or capillary dies. While there have been many studies of extrudate swell of molten polymers and its variation with process conditions,[17–27] few of these studies deal with the influence of molecular weight distribution[21,23,25,26] and apparently none of these with such effects in polypropylene. We present such an investigation here.

The present paper is a continuation of earlier associated studies on polypropylene of the influence of molecular weight distribution on rheological properties[28] and of dynamics and structure development in melt spinning.[29,30] It also continues our investigations of the influence of rheological properties on melt spinning behavior.[1,12,24,31]

EXPERIMENTAL

Materials

A series of seven polypropylenes of varying molecular weight and distribution were supplied by the polypropylene division of Diamond Shamrock (now part of ARCO). These polymers and their characterization are summarized in Table I. In an earlier study[28] we presented shear and elongational viscosity and principal normal stress difference data for these melts at 180°C.

TABLE I
Samples (Polypropylene)[a]

Code	Melt index	$M_w \times 10^{-5}$	M_w/M_n	M_z/M_w	$M_v \times 10^{-5}$
PP-H-N	4.2	2.84	6.4	2.6	2.40
PP-H-R-B	5.0	3.03	9.0	3.6	2.42
PP-H-B-R	3.7	3.39	7.7	3.6	2.71
PP-M-N	11.6	2.32	4.7	2.8	1.92
PP-M-B	11.0	2.68	9.0	4.45	2.07
PP-L-N	25.0	1.79	4.6	2.5	1.52
PP-L-R-N	23.0	2.02	6.7	3.2	1.66

[a] H: High molecular weight; M: middle molecular weight; L: low molecular weight; N: narrow molecular weight distribution; R: regular molecular weight distribution; B: broad molecular weight distribution.

Isothermal Melt Spinning Apparent Spinline Elongational Viscosity Measurements

The melt spinning of the polypropylenes was carried out at 180°C using an Instron capillary rheometer as a delivery device (Fig. 1). The polymer was extruded at 180°C through a die of diameter 0.029 in. and length/diameter ratio of 53.88. The extrudate directly passes into a 1.0-in. inside diameter and 3.0-in.-long heated chamber and finally into a water quench bath. Two sets of electrical heaters were used to heat the chambers. One set was controlled by a thermocouple 0.25 in. from the die exit and the other set by a thermocouple placed halfway down the length of the chamber. The take-up roll, which had a diameter of 6.35 cm, was driven by a 1/15 horsepower B and B motor (12 rpm maximum speed). A take-up velocity of 0.72 to 0.78 m/min was used with a volumetric throughput of 9.05×10^{-2} cm^3/min.

A Rothschild tensiometer was placed near the take-up device to measure the spinline tension. However, the presence of a pair of Teflon rods in the bath and between the bath and the tensiometer necessitates further calibration. If F_L is the force in the absence of the Teflon rods, F_{rheo} is the force acting on the melt in the spinline, F_{drag} is the drag force, F_{grav} is the gravitational force, and F_{inertia} is the inertial force, then[32]

$$F_{\text{rheo}} = F_L + F_{\text{grav}} - F_{\text{drag}} - F_{\text{inertia}} \tag{1}$$

And if F_T is the tension measured in the presence of the rods,[33]

$$F_L = F_T\, e^{-\alpha_1\theta_1}\, e^{-\alpha_2\theta_2} \tag{2}$$

where α_1 and α_2 are friction coefficients and θ_1 and θ_2 the angles of contact with the rods. The quantities F_{grav} and F_{inertia} can be directly calculated from dimensions and velocities; F_{drag} may be estimated using the many correlations in the literature.[32] We have used the work of Sano and Orii.[34] The quantity $e^{-\alpha_1\theta_1}$

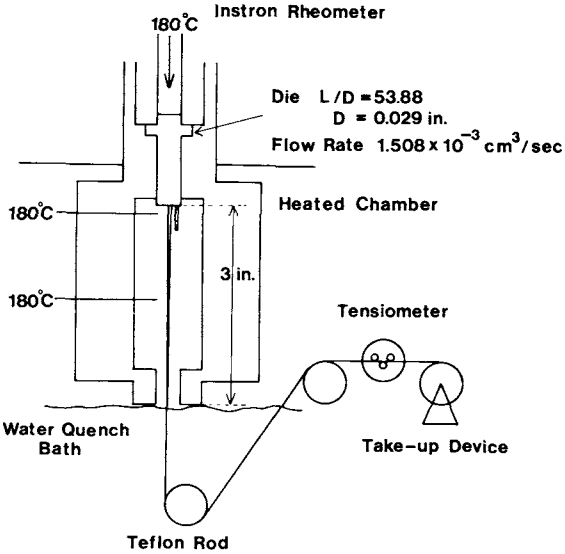

Fig. 1. Apparatus for isothermal melt spinning and measurement of elongational viscosity.

$e^{-\alpha_2\theta_2}$ can be estimated by replacing the spinline with a solidified fiber being held in tension by weight W as shown in Figure 2. It follows that

$$F_T = W\, e^{\alpha_A\theta_A}\, e^{\alpha_B\theta_B}\, e^{\alpha_1\theta_1}\, e^{\alpha_2\theta_2} \tag{3}$$

The tensiometer may also be placed in front of the water bath. This allows evaluation of $e^{\alpha_A\theta_A}\, e^{\alpha_B\theta_B}$.

The above computations show that F_{grav} is of order 0.015 to 0.024 g at the die exit and decreases to zero in spinline. F_{drag} is of the order of 0.006 g at the low speeds of the study. F_{inertia} is still smaller. The quantity $e^{-\alpha_1\theta_1}\, e^{-\alpha_2\theta_2}$ is close to unity, with $e^{-\alpha_1\theta_1}\, e^{-\alpha_2\theta_2} - 1$ being less than 0.01.

Photographs were taken to measure the changing diameter along the spinline. A Nikon SLR-type camera with a 135-mm lens mounted on a bellows for maximum enlargement was used. Bright spotlights were located just below the camera. The resulting slides were enlarged by a slide projector in order to make measurements of the diameter profile by comparing the extrudate with a reference scale. Data were taken between 0.6 and 4.0 cm from the die exit.

The spinline elongational viscosity was calculated from

$$\chi_{sp} = \frac{\sigma_{11}}{dv_1/dx_1} = \frac{F_{\text{rheo}}/(\pi d^2/4)}{(d/dx_1)(4Q/\pi d^2)} \tag{4}$$

where d is the fiber diameter at position x_1; Q is the volumetric flow rate; and σ_{11} and dv_1/dx_1 are the local stress and elongation rate, respectively. It is necessary to differentiate the diameter profile with respect to distance.

Fiber Diameter Variations in Melt Spinning

The same experimental setup as described above was used in the isothermal melt spinning experiments. For nonisothermal melt spinning, the isothermal chamber was removed and a die 0.058 in. in diameter and L/D ratio of 10 was used. The spinpath was maintained at 19.5 cm. The development of diameter variations along the fiber was detected by tensiometer measurements. Fiber diameter profiles and amplitudes and wavelengths of diameter fluctuations were measured using a profile projector (model #P01 LP-6, Ehrenreich Photo-optical Industries, Inc., Garden City, NY).

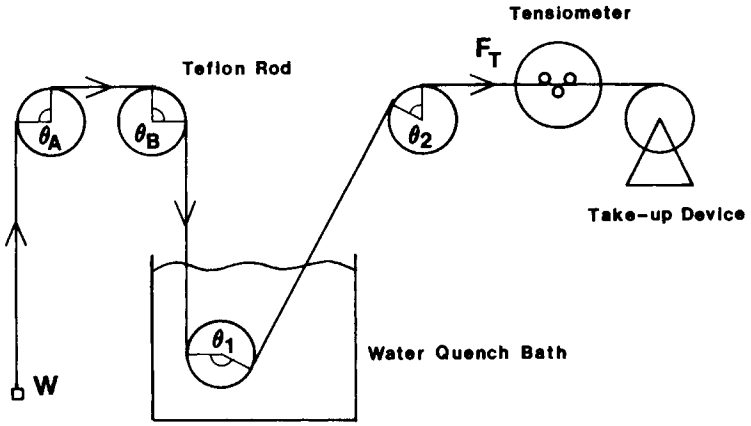

Fig. 2. Calibration of melt-spinning tension measurements.

Extrudate Swell

Extrudate swell measurements were made at 180°C using an Instron capillary rheometer with a die having a diameter of 0.058 in. and a die L/D ratio of 40. Based on experimental results of earlier investigators,[20,24] this is equivalent to infinite die length. The descending filaments were cut with scissors at a distance of 2 in. below the die (except at the lowest extrusion rates $\dot{\gamma}_w < 0.5\ \text{sec}^{-1}$, where a distance of 0.5 in. was used) and placed in a bath of polyethylene glycol (Union Carbide Carbowax PEG 400) at 110°C for a period of 30 min. This is 50°C below the melting temperature. This treatment would tend to heal voids and bring all the filaments to the same structural condition. There is, however, none of the unconstrained recovery which occurs if the sample is annealed above its melting temperature.[22,24]

The extrudates were later annealed at 180°C in silicone oil for 5 min. This allowed estimation of the total recovery.[24]

ISOTHERMAL MELT SPINNING

Results

We plot the velocity profiles, $v_1(x_1) = Q/\pi d^2/4$, for the descending fibers for the four polypropylenes in Figure 3. It may be seen that the two broad-distribution samples (PP-M-B, PP-H-R-B) are being drawn down more rapidly than the narrow-distribution polymers (PP-H-N, PP-M-N). The velocities of the broader-distribution samples increase more rapidly with distance than the narrower-distribution samples. This is seen in the elongation rate profiles of Figure 4. The more rapidly increasing elongation rate, $E = dv_1/dx_1$, for the former polymers implies a more rapidly decreasing or less rapidly increasing "apparent" elongational viscosity.

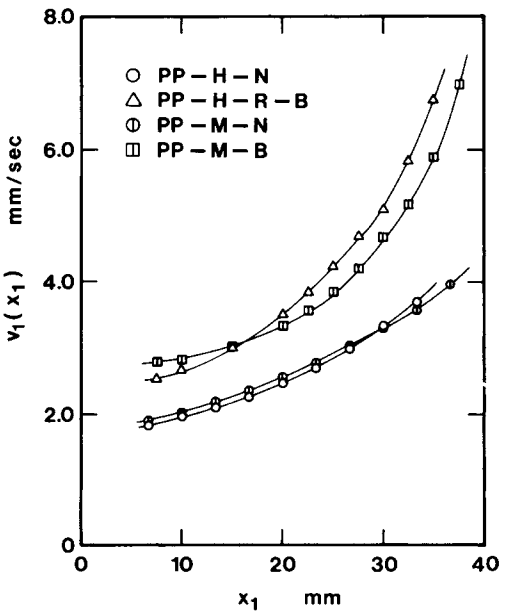

Fig. 3. Velocity profiles of polypropylene fibers during melt spinning for four polypropylenes.

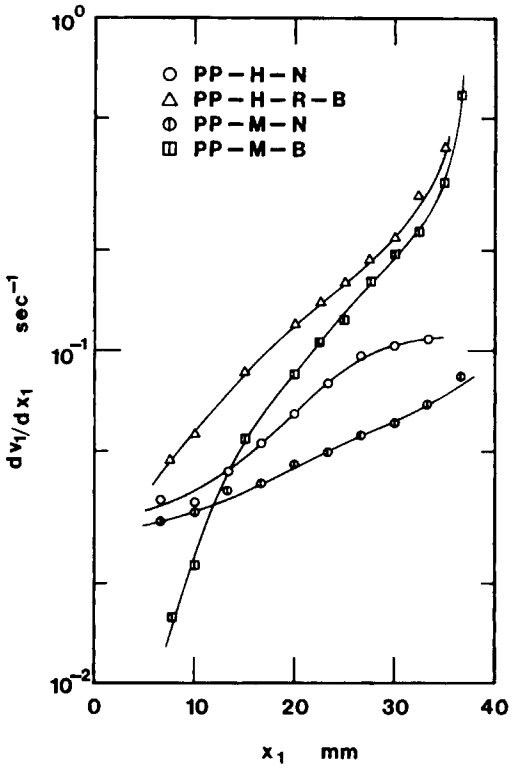

Fig. 4. Local elongation rate vs. spinline position for four polypropylenes.

The experimentally determined apparent elongational viscosity is plotted as a function of local spinline elongation rate in Figure 5. It may be seen that the function χ_{sp} decreases with increasing deformation rate, but the rate of decrease varies from polymer to polymer. Comparing the results of this figure with the

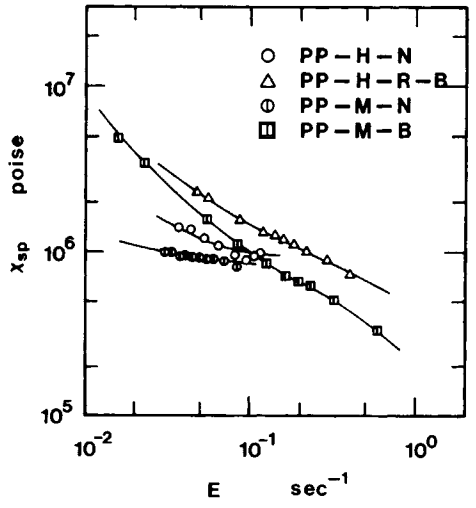

Fig. 5. Apparent melt spinning elongational viscosity as function of elongation rate for polypropylene.

molecular weight data of Table I, we see that χ_{sp} increases with average molecular weight, but its rate of decrease increases with breadth of molecular weight distribution.

Discussion of Results

It is of interest to contrast the apparent melt spinning elongational viscosity with the results of more basic experimental studies. We have carried out such measurements in an earlier study.[28] In Figure 6 we compare the results of elongational viscosities determined from local point by point spinline measurements and from simple elongational flow. For the PP-H-N and the PP-M-N, the χ values from the simple elongational flow experiments are equal to $3\eta_0$ at low elongation rates and increase at higher rates of deformation. However, the results of the melt spinning experiments show an elongational viscosity decreasing with elongation rate. For the broader-distribution polypropylenes, both experiments yield an elongational viscosity which decreases with elongation rate. The apparent elongational viscosity from the melt spinning experiments decreases more rapidly. It also appears that the melt spinning elongational viscosities are generally larger in magnitude.

Other investigators have measured apparent elongational viscosities using isothermal melt spinning.[1-4] We summarize these data in Figure 7. Generally our data on the broader-distribution polypropylenes are similar to those of Han and Lamonte[2] on a commercial polypropylene. The dependence of χ_{sp} on molecular weight distribution would seem compatible with the earlier observation of Han and Lamonte[2] on a series of rather broad-distribution high-density polyethylenes.

It is also of interest to consider the implications of our studies on the melt

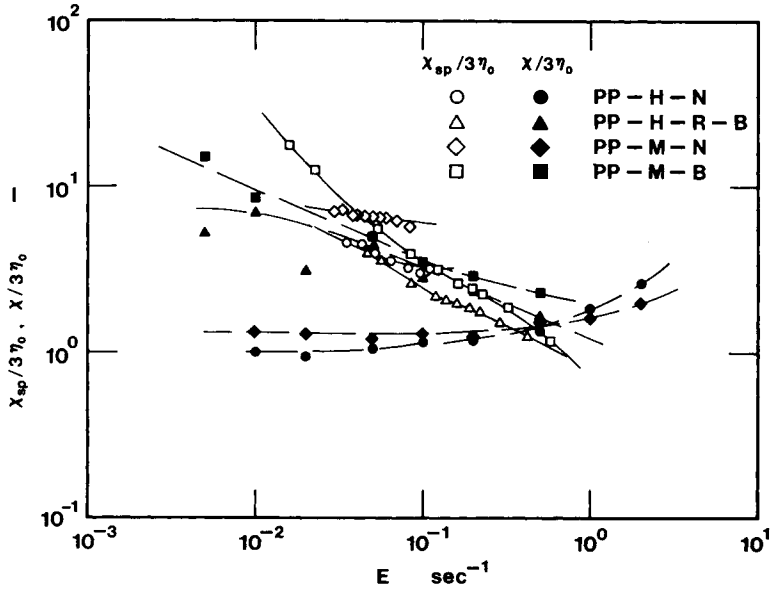

Fig. 6. Elongational viscosity measured by melt spinning and by constant elongational rate experiments.

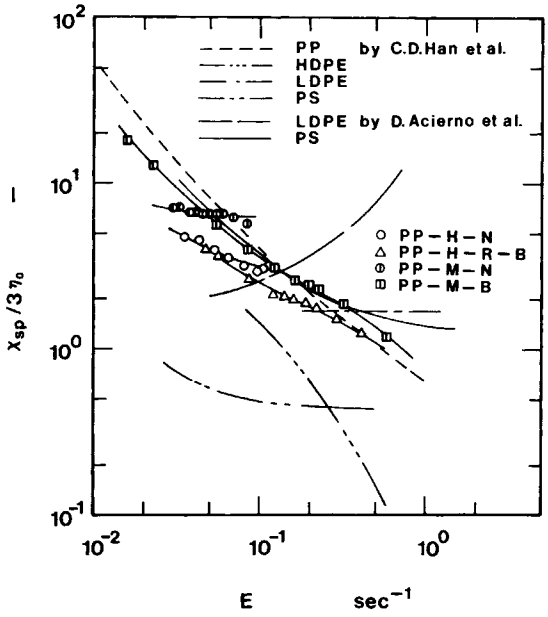

Fig. 7. Melt spinning elongational viscosities from the literature. Data from Acierno et al.[1] and Han and Lamonte[2] is included.

spinning elongational viscosities χ_{sp} of polymer melts in general. From Figure 7 we see that the spinline elongational viscosities of commercial polystyrene (PS) melts decrease with elongation rate. However, experiments were carried out on similar virgin PS filaments in simple constant elongation viscosities which equal $3\eta_0$ at low deformation rates and then increase at higher rates of deformation.[35–37] The studies of melt spinning elongational viscosity of low-density polyethylene (LDPE) by Acierno et al.[1] show an increasing function, while the investigation of Han and Lamonte[2] indicate a constant value. Investigators using constant elongation rate experiments generally find LDPE exhibits an increasing elongational viscosity,[31–39] though Laun and Munstedt[40] find that the elongational viscosity reaches a maximum and then decreases. From comparing these melt spinning and elongational viscosity data on PS and LDPE and our own previously cited studies on polypropylenes, it would seem that the melt spinning or apparent spinline elongational viscosity has a lower (or more negative) slope than the simple elongational-flow steady-state viscosity, and a larger magnitude.

Comparison to Theories of Melt Spinning

The modeling of melt spinning processes dates to the researches of Ziabicki and Kedzierska[41] and Kase and Matsuo.[8,16,42] These researchers, however, considered the polymer melts to behave as Newtonian fluids in the threadline. Later investigators such as Lamonte and Han[43] attempted to improve this modeling by presuming the melt to obey a power law elongational viscosity. However, since polymer melts are viscoelastic fluids, any proper modeling should

take this into consideration. The first study of the melt spinning process which properly considers the viscoelastic characteristics of the melt is that of Acierno, Dalton, Rodriquez, and White,[1] who also compare experiment with predictions based on rheological characterization of the melt. These authors consider isothermal melt spinning and base their analysis on an integral fluid model. This work was subsequently extended by Chen et al.[31] and has led in more recent times to the general formulation of Matsui and Bogue,[44] which is the most sophisticated study to date. Matsui and Bogue include a careful treatment of nonisothermal behavior of the polymer melt (see the related work of Bogue et al.[45]) and the influence of flow in the spinneret. A more recent study by Denn and Marrucci[46] considers the Acierno et al.[1] formulation of this problem but gives emphasis to the influence of the form of the relaxation spectrum. A useful critique is given by Petrie.[47]

The basic problem with the integral constitutive equation formulation is its complexity. It is desirable to be able to use a simpler model for such analyses. Zeichner[48] has shown that such a theory can be developed from the convected Maxwell model. This view has been taken in succeeding papers by Denn, Petrie, and Avenas,[49] Fisher and Denn,[50] Petrie,[47] Chang and Denn,[51] and White and Ide.[12] The results of these investigators, especially the latter, may be used to interpret our results.

If we begin with the convected Maxwell (White–Metzner) model constitutive equation,[12,28,48–55]

$$\sigma = -p\mathbf{I} + \mathbf{P} \tag{5a}$$

$$\tau \frac{\delta \mathbf{P}}{\delta t} = 2G\tau\mathbf{d} - \mathbf{P} \tag{5b}$$

where $\mathbf{P}$ is the extra stress, $\mathbf{d}$ is the rate of deformation tensor, and G and τ parameters where τ is a function of II_d the second invariant of $\mathbf{d}$. This may usefully be taken as[12,28,53]

$$\tau = \frac{\tau_0}{1 + a\tau_0 \mathrm{II}_d{}^{1/2}} \tag{6}$$

Minoshima et al.[28] interpret their experimental studies of molecular weight distribution effects on elongational flow using eqs. (5) and (6). Broadening the molecular weight distribution decreases G (increasing steady-state compliance) and increases a. Values of a from Minoshima et al. are given in Table II. In the studies of Fisher and Denn[50] and Chang and Denn,[51] power law forms are used to represent deformation rate dependence of τ (and G). This is unsatisfactory because it leads to improper low deformation rate behavior.

For isothermal melt spinning,[12,48–50]

$$v_1 = v_1(x_1) \tag{7a}$$

$$v_2(x_2) = v_3(x_3) \tag{7b}$$

$$\frac{\partial v_1}{\partial x_1} + \frac{\partial v_2}{\partial x_2} + \frac{\partial v_1}{\partial x_3} = 0 \tag{7c}$$

$$F = \sigma_{11}\pi R^2 = (P_{11} - P_{22})\pi R^2 = (P_{11} - P_{22})\frac{Q}{v_1} \tag{8}$$

TABLE II
Molecular Weight Distribution, a Value, and Onset of Draw Resonance: Isothermal and Nonisothermal Melt Spinning

Material	M_w/M_n	a*	Onset of draw resonance V_L/V_0	
			Isothermal melt spinning into quench bath	Nonisothermal melt spinning into quench bath
PP-H-N	6.4	0.7	7.0	22.0
PP-H-R-B	9.0	1.2	3.6	10.0
PP-M-N	4.7	0.6	7.7	19.0
PP-M-B	9.0	1.2	4.3	9.0
PP-L-R	4.6	0.7	—	23.0
PP-L-R-N	6.7	0.9	—	19.0

* Best fit from sheer viscosity, principal normal stress difference, and elongational viscosity.

and eq. (5) may be written

$$\tau\left(v_1\frac{\partial P_{11}}{\partial x_1} - 2P_{11}\frac{\partial v_1}{\partial x_1}\right) = 2G\tau\frac{\partial v_1}{\partial x_1} - P_{11} \tag{9a}$$

$$\tau\left(v_1\frac{\partial P_{22}}{\partial x_1} + P_{22}\frac{\partial v_1}{\partial x_1}\right) = -G\tau\frac{\partial v_1}{\partial x_1} - P_{22} \tag{9b}$$

We follow now the analysis of White and Ide.[12] If we take P_{11} to dominate P_{22} and neglect the latter (Zeichner's asymptote), eq. (9b) may be neglected and eq. (9a) solved to give

$$\frac{F}{Q}[x_1 + (\sqrt{3}a - 1)\tau_0[v_1(x_1) - v_1(0)]] = 2G\tau_0 \ln\frac{v_1(x_1)}{v_1(0)} \tag{10}$$

which may be rearranged to give an apparent spinline elongational viscosity of

$$\chi_{sp} = \frac{\sigma_{11}}{dv_1/dx_1} = \frac{2G\tau_0}{1 + (\sqrt{3}a - 1)\tau_0 dv_1/dx_1} \tag{11}$$

Taking τ_0 equal to zero at nonzero $G\tau_0$ gives the Newtonian value of χ_{sp} of $2G\tau_0$, or $2\eta_0$. The reason for the 2 rather than 3 comes from neglect of eq. (9b). We should note at this point that Petrie[47] has shown that in general one cannot define a χ_{sp} (dv_1/dx_1) and that this is specifically the case if eq. (9b) is included. However, despite this, the procedure of this paper is a good approximation.

Certain conclusions may be drawn from eq. (10). At a value of a equal to $1/\sqrt{3}$, the velocity profile in the spinline is exponential as with a Newtonian fluid. For smaller a or large τ_0 it tends to become linear with

$$\frac{v_1(x)}{v_1(0)} = 1 + \frac{1}{(1 - \sqrt{3}a)}\frac{1}{N_{Ws}}\frac{x_1}{L} \tag{12}$$

where N_{Ws} is a Weissenberg number, $\tau_0 v_1(0)/L$.[53–55] This is what is observed in Figure 3.

If we consider a constant elongation rate stretching flow and determine χ for the model of eqs. (5), (6), and (9) but which neglects eq. (9b), we obtain

$$\chi = \frac{2G\tau}{1 - 2\tau E} \tag{13}$$

where E is dv_1/dx_1 with

$$\tau = \frac{\tau_0}{1 + \sqrt{3}a\tau_0 E} \tag{14}$$

giving

$$\chi = \frac{2G\tau_0}{1 + (\sqrt{3}a - 2)\tau_0 E} \tag{15}$$

Comparing eqs. (15) and (11), we see that the criterion for χ or χ_{sp} to be an increasing (or decreasing) function of elongation rate differs. In both cases increasing a tends to make χ a decreasing function. The criterion for χ_{sp} is more severe. If a is greater than $1/\sqrt{3}$ (i.e., 0.58), χ_{sp} will be a decreasing function. For χ the criterion is $2/\sqrt{3}$ (1.15). For the narrow molecular weight distribution PP, the value of a is in this intermediate range, giving an increasing χ and a decreasing χ_{sp}. The broader-distribution samples have larger a and give both decreasing χ and χ_{sp}.

The above conclusions may be used to explain some of the perplexing results of Acierno et al.[1] and Han and Lamonte.[2] They find that χ_{sp} is a decreasing function of elongation rate for PS melts which give an increasing χ,[35–37] while the latter authors find χ_{sp} to be a constant in one case for LDPE which has an increasing χ.[37–39] The χ_{sp} character of LDPE and PS (as well as HDPE) depends on the a parameters listed in Table III. Only LDPE has a low enough value of a to lead to a constant or increasing χ_{sp}. Similar remarks would appear to be valid for the nylon 6 investigated by Bankar, Spruiell, and White.[4] It has an a of 0.15 and an increasing χ_{sp} function.

The analysis given above yields imperfect results in some important ways. The ratio χ_{sp}/χ taken from eqs. (11) and (15) is predicted to be less than unity. From Figure 6 we see that χ is more often smaller, especially for the narrow-distribution samples. Indeed at low $\tau_0 E$, the latter is most notably the case. Furthermore, the χ_{sp} data do not go to the Newtonian asymptote at low elongation rates. The values are too high. However, this is also the case for χ in melts with large a. The problem is probably due in part to eq. (16) being an imperfect choice for the $\tau(\mathrm{II}_d)$ function. We also should include the P_{22} term, eq. (9b), in our analysis. However, it is to be noted that other investigators have found that the stress values in melt spinning experiments are too high and that to predict them from shear flow higher values of the moduli or equivalent would have to be used in the constitutive equation. Chang and Denn[51] report such findings in experiments on a polyacrylamide dissolved in corn syrup (shear viscosity of 200 poise at 1

TABLE III
Range of a Values for Various Commercial Polymers and Melt Spinning Behavior

Material	a	χ_{sp}	Draw resonance
LDPE	0.2–0.6	constant or increases	does not occur
Nylon 6	0.15	increasing	—
PS	0.7	decreasing	moderate V_L/V_0
HDPE	1.2–1.4	decreasing	low V_L/V_0
PP	1.2	decreasing	low V_L/V_0

sec^{-1}) based on calculations using a convected Maxwell model of the type in eq. (5) where they include eq. (9b) and use power law deformation rate dependence of τ and G. They suggest the inadequacy is due to failure to include the spectrum of relaxation times. Chen et al.,[31] however, report similar difficulties using an integral model.

FILAMENT UNIFORMITY

Results

At the start of the melt spinning process, the descending extrudate is pulled onto the take-up roll. It was found that all polymers, especially the moderate and broad molecular weight distribution samples, have to be pulled very carefully to avoid ductile failure which occurs somewhere between the extrudate swell region and the middle of the spinline.

After the steady-state spinline has been achieved, extrudate diameter fluctuations of two types are observed. One of these is random in character and seems to occur to varying extents under all spinning conditions in which the threadline is drawn down. It is to be emphasized that this behavior is not a die flow instability as we have studied such conditions carefully (see next section). It is also not due to fluctuations in the extrusion system as we are using a constant volumetric throughput rate apparatus. The second type of diameter fluctuation has a well-defined wavelength or period and a much larger amplitude. The two types of diameter fluctuations are illustrated in Figure 8. Here, the diameter reduced by the average filament diameter versus distance along the solidified filament is plotted.

The onset of the second type of diameter fluctuation was investigated for both the isothermal (temperature chamber in place) and nonisothermal spinning conditions. The critical drawdown ratio V_L/V_0 is summarized in Table II for

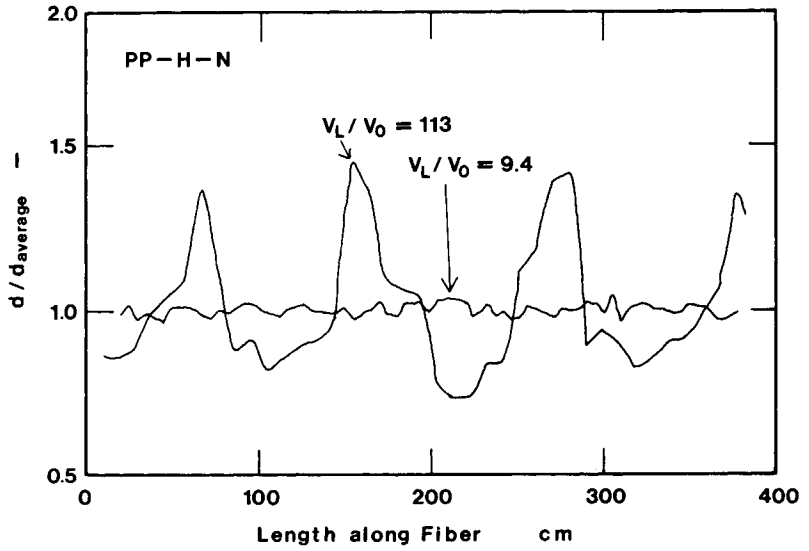

Fig. 8. Diameter fluctuations for polypropylene fibers, random fluctuation, and fluctuation of well-defined wavelength under nonisothermal condition.

both cases. Removal of the temperature chamber stabilizes the spinline and increases the critical drawdown ratio.

Interpretation

It would appear that there are two separate phenomena giving rise to fluctuations in filament diameter in the threadline. There are fluctuations brought on by system disturbances as proposed by Kase and Matsuo,[7] which may be termed "forced oscillations." Secondly, there is "draw resonance" or "natural oscillations." This latter phenomenon was first analyzed by Kase, Matsuo, and Yoshimoto[16] and has since been treated by various investigators.[8,9,11,12,50,56–59] The former phenomenon has received treatment for the case of a nonisothermal Newtonian fluid only. The latter, where work is more extensive, has received attention for an isothermal Newtonian fluid,[16,56] isothermal power law fluid,[11,57] isothermal viscoelastic fluid represented by a convected Maxwell model,[50,51] and various nonisothermal models.[9,58,59]

From analyzing the various papers listed above, it would seem that modifying any rheological model in such a way as to give the true or apparent spinline elongational viscosity versus elongation rate relationship a lower slope results in draw resonance occurring at lower drawdown ratios. Following White and Ide's formulation,[12] the a parameter represents this deformation rate softening. Clearly, as a increases (see Table II), the spinline destabilizes and the critical V_L/V_0 decreases. Analyzing Kase and Matsuo's formulation[7] leading to forced oscillations, it would seem clear that a similar influence on the spinline elongational viscosity function would lead to accentuation of the diameter fluctuations.

White and Ide[12] argue that draw resonance is a continuous spinline form of the neck development ductile failure instability.[53] Polymer melts exhibiting ductile failure should tend to exhibit draw resonance at low V_L/V_0. Comparing the results of Table II with the data of Minoshima et al.,[28] we find that this is indeed the case.

From the above considerations it would seem clear that as narrowing the molecular weight distributions of polypropylene causes the slope of the spinline elongational viscosity-versus-elongation rate curve to increase, one should expect a more stable spinline for these materials. The intensity of diameter fluctuations due to forced oscillations should be less and the drawdown required to obtain draw resonance increased. This is what is observed.

EXTRUDATE SWELL

Results

We plot the extrudate swell B as a function of die wall shear rate in Figure 9, where B is d/D, the ratio of extrudate to die diameter. Generally, swell for each melt increases with die wall shear rate. The level of the swell is a strong increasing function of breadth of molecular weight distribution. In Figure 10 we replot the data as a function of die wall shear stress. The distinctions in the data are reduced somewhat, but the same trends exist as in Figure 9.

The influence of annealing is shown in Figure 11, where B_a is the ratio of an-

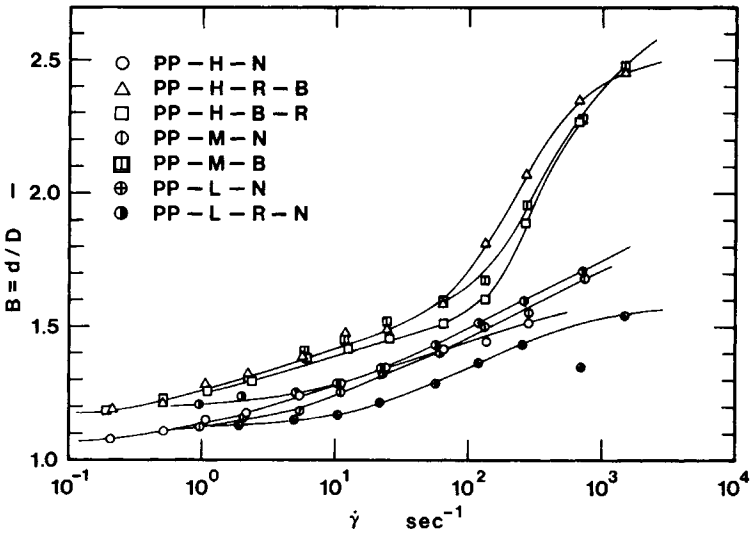

Fig. 9. Extrudate swell as function of die wall shear rate.

nealed extrudate to die diameter. The broader molecular weight distribution samples exhibit significantly greater delayed recovery.

Interpretation

It should first be noted that extrudate swell results are difficult to reproduce and strongly depend on the detailed technique used in their measurement. Some of the problems involved are considered in our earlier papers.[24,27] Generally, our data give slightly higher values of B on a given polymer than those reported by Huang and White.[27]

The theoretical problem of extrudate swell can be approached at many levels

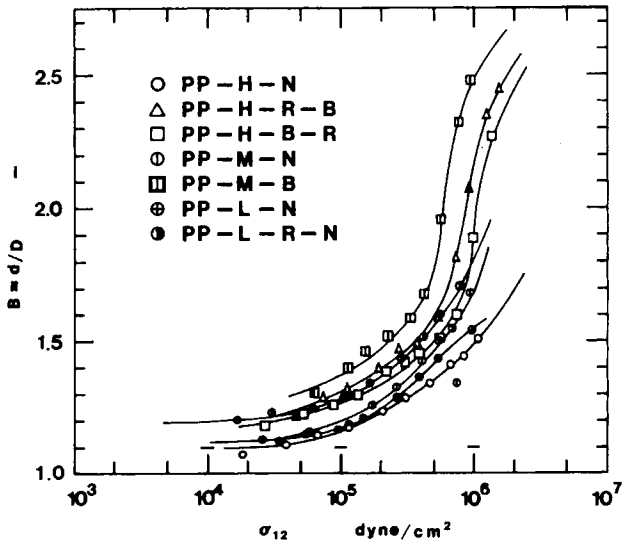

Fig. 10. Extrudate swell as function of die wall shear stress.

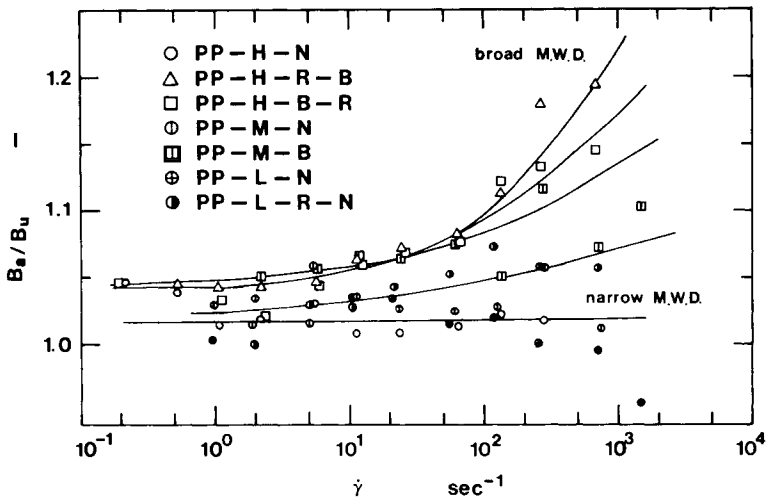

Fig. 11. Delayed recovery as function of die wall shear rate.

of sophistication. From a simplistic point of view, extrudate swell is simply an averaged elastic recovery S from the shear stress σ_{12} in Poiseuille flow. This idea is expressed by Nakajima and Shida[20] and many later investigators. It follows that

$$B \sim \bar{S} \sim \overline{\sigma_{12}}/G \sim J_e \overline{\sigma_{12}} \tag{16}$$

J_e is a strongly increasing function of breadth of molecular weight distribution.[28] One should thus expect the molecular weight distribution effects of Figure 10 relating B and $(\sigma_{12})_w$.

From the theory of the convected Maxwell model of eq. (5)

$$N_1 = 2\sigma_{12}^2/G \tag{17}$$

so that

$$B \sim N_1/(\sigma_{12})_w \tag{18}$$

A similar result can be obtained from dimensional analysis arguments. If a viscoelastic fluid's rheological behavior is specified by a Maxwell model (with a constant relaxation time τ), the velocity fields are specified by the dimensionless group, the Weissenberg number,[53-55]

$$N_{Ws} = \tau U/L \tag{19}$$

where U and L are the characteristic velocity and length. Thus,

$$B \sim N_{Ws} \tag{20}$$

In a laminar shear flow of a convected Maxwell fluid, we have from eq. (22)

$$N_1 = 2\eta\tau\dot{\gamma}^2 \qquad (\tau = \eta/G) \tag{21}$$

If we take U/L as $\dot{\gamma}_w$, it follows that we obtain*

$$B \sim N_{Ws} = N_1/2\sigma_{12} \sim \bar{S} \tag{22}$$

* The original treatment[60] of the Weissenberg number was in terms of the second-order fluid[61] and emphasized its relationship to swell.

The simplest consistent theory of the extrudate swell of a Maxwell fluid with constant τ is that developed by Tanner[62] based on unconstrained recovery from Poiseuille flow from a very long tube. This leads to

$$B = \left[1 + \frac{1}{8}\left(\frac{N_1}{\sigma_{12}}\right)_w^2\right]^{1/6} \tag{23}$$

A constant of 0.1 is generally added to account for the observed swell of a Newtonian fluid.

Equations (20), (22), and (23) suggest that we attempt to correlate B with the ratio of N_1/σ_{12} evaluated at the die wall. This is done in Figure 12. N_1 is evaluated by extrapolation of $N_1(\sigma_{12})$ data using a power law equation. There are of course great difficulties with this procedure and it can only be considered approximate. It is found that there is still a molecular weight distribution effect, with B being larger for broader-distribution melts. This agrees with the finding of Racin and Bogue[26] for polystyrene melts. Generally, eq. (23) (even with the added 0.1) underpredicts the value of B, even for the narrower-distribution samples.

If we consider more general viscoelastic fluid models, the Weissenberg number is still the primary dimensionless group, but the definition of τ is ambiguous. We may of course arbitrarily define τ through eq. (21). Other dimensionless groups arise, representing the form of the relaxation spectrum and other nonlinearities which arise. These groups, however, do not contain U or L. These groups have been referred to as "viscoelastic ratio numbers."

If we retain the Maxwell model form but allow τ to depend upon deformation rate as in the form frequently used in the literature,[28,57,58] we would predict

$$B = F[N_{Ws}, \tau(\dot{\gamma})/\tau_0] \tag{24}$$

but the derivation leading to eq. (23) is unchanged. Racin and Bogue[26] and Huang and White[27] consider the special case

$$N_1 = A\sigma_{12}^{\alpha} \tag{25}$$

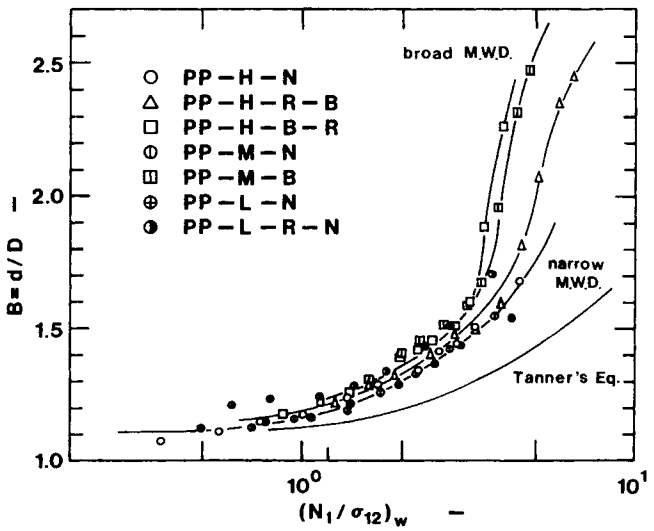

Fig. 12. Extrudate swell as function of $(N_1/\sigma_{12})_w$.

which implies a $\dot{\gamma}$- or σ_{12}-dependent modulus in the Maxwell model, which results in eq. (23) being modified to

$$B = [1 + f(\alpha)(N_1/\sigma_{12})^2]^{1/6} + 0.1 \tag{26}$$

From experimental studies of normal stresses, α decreases with increasing distribution breadth. This result predicts an increase in B, but not enough to correlate the data. However, the latter comment may in part be due to problems of experimental techniques indicated in the first paragraph of this section.

If one goes back to the original Tanner extrudate swell theory[62] based on unconstrained recovery, one observes that the theory does not include the distribution of relaxation times. The necessity of including multiple time constants is supported by the existence of delayed recovery, which is shown in Figure 11.

CONCLUSIONS

An experimental study of the influence of molecular weight distribution on the melt spinning and extrudate swell characteristics of PP has been reported:

1. The spinline elongational viscosity χ_{sp} measured by isothermal melt spinning behaves roughly similar to χ obtained from a constant deformation rate apparatus. χ_{sp} of narrow molecular weight distribution PP decreases slightly with increasing dv_1/dx_1, while for broad molecular weight distribution PP it decreases rapidly with increasing dv_1/dx_1. χ is an increasing function of deformation rate for the narrower samples and a decreasing function for the broader-distribution polymers.

2. The different behavior of χ_{sp} and χ is interpreted using a convected Maxwell model. The different slopes of χ_{sp} and χ functions of dv_1/dx_1 can be explained in terms of the deformation rate dependence of τ. A problem exists in predicting relative magnitudes with χ_{sp} being larger than expected.

3. Broad molecular weight distribution PP more readily exhibits draw resonance compared to narrow molecular weight distribution PP under both isothermal and nonisothermal conditions. This can be explained by theories of the draw resonance instability in non-Newtonian and viscoelastic fluids through the influence of molecular weight distribution on the elongational viscosity function.

4. Broadening of the molecular weight distribution increases extrudate swell at fixed shear rate, shear stress, and Weissenberg number $N_{Ws} = N_1/2\sigma_{12}$.

5. Broad molecular weight distribution PP has a larger delayed recovery than narrow molecular weight distribution PP.

6. It is suggested that narrow molecular weight distribution PP should be preferentially used for processing which is based upon uniaxial elongational flow.

APPENDIX

Implications of Melt Spinning Behavior for Structure Development and Mechanical Properties

The orientation of the polymer chains in a melt in a spinline may be represented by its birefringence. In the molten state, polypropylene and other polymer melts obey the rheo-optical law.[63] In a fiber spinline this states that the birefringence $n_1 - n_2$ is proportional to the stress, i.e.,[64]

$$n_1 - n_2 = \Delta n = C\sigma_{11} \tag{A-1}$$

The second moment of the mean orientation of polymer chain segments $\overline{\cos^2\theta}$, where θ is the angle between segment and fiber axis, is related to the ratio of the birefringence and the maximum or intrinsic birefringence Δ^0 through[65]

$$f = \frac{\Delta n}{\Delta^0} = \frac{3\,\overline{\cos^2\theta} - 1}{2} \tag{A-2}$$

where f is known as the Hermans orientation factor. The ratio C/Δ^0 appears to be a constant independent of (flexible chain) polymer type,[64] so that f would seem to be a unique function of the spinline stress, i.e.,

$$f = \frac{C}{\Delta^0}\sigma_{11} \tag{A-3}$$

Polypropylene crystallizes when it is melt spun. Nadella, Henson, Spruiell, and White[29,30] investigated the structure of melt-spun polypropylene fibers and using WAXS measurements determined the orientation factors f_a, f_b, and f_c (chain axis) for the three crystallographic axes, defined as in eq. (A-2) but using angles θ_j between the fiber and crystallographic axes. They showed that the orientation factors for a series of polypropylenes of varying molecular weight and distribution melt spun under a range of different conditions were a unique function of the spinline stress.[30] This clearly results from the f_a, f_b, and f_c being determined by the f of eqs. (A-2) and (A-3):

$$f_j = F_j[f] = F_j\left[\frac{C}{\Delta^0}\sigma_{11}\right] \tag{A-4}$$

The birefringence of the crystalline melt-spun fibers which is the sum of contributions of crystalline and amorphous phases[66–69]

$$\Delta n = Xf_c(\sigma_{11})\Delta^0_{\text{cryst}} + (1 - X)f_{\text{amorph}}(\sigma_{11})\Delta^0_{\text{amorph}} \tag{A-5}$$

where X is the fraction of crystallinity, Δ^0_{cryst} and Δ^0_{amorph} are the intrinsic birefringence of the crystalline and amorphous phases, and f_{amorph} is the Hermans orientation factor in the amorphous regions.

Returning now to the polypropylenes of varying molecular weight distribution which were investigated in this paper, the different melt spinning elongational viscosity functions will result in different spinline stresses being required to achieve a specific drawdown. At moderate and higher drawdown ratios, the data of Figure 5 suggest that higher stress levels will be required for the narrower-distribution polymers at the same zero shear or higher shear rate viscosities. These will lead to higher spinline birefringences and higher spun fiber birefringences and crystalline orientation.

The mechanical properties of the melt-spun fibers are determined by the crystalline morphology and orientation. The Young's modulus, yield stress, tensile strength, and elongation to break may be correlated with the birefringence and with the Hermans orientation factors of the crystalline and amorphous phases.[30,69,70] Not surprisingly from eqs. (A-4) and (A-5), Nadella et al.[30] found a good correlation between mechanical properties and spinline stress. It would thus appear that for polymers with the same level of low shear rate melt viscosity which were spun under the same set of kinematic conditions, the narrower molecular weight distributions will develop not only high spinline stresses and birefringence but increased Young's modulus and tensile strength as well as reduced elongation to break. The latter effect could give rise to problems in subsequent drawing operations.

This work was supported in part by Diamond Shamrock Corporation and ARCO. The authors especially thank T. H. Bragg who gave continued interest and encouragement. The work was also supported in part by the National Science Foundation under Grant NSF ENG 75-16974.

References

1. D. Acierno, J. N. Dalton, J. M. Rodriguez, and J. L. White, *J. Appl. Polym. Sci.*, **15**, 2395 (1971).
2. C. D. Han and R. R. Lamonte, *Trans. Soc. Rheol.*, **16**, 447 (1972).
3. V. G. Bankar, J. E. Spruiell, and J. L. White, *J. Appl. Polym. Sci.*, **21**, 2135 (1977).
4. J. W. Hill and J. A. Cuculo, *J. Appl. Polym. Sci., Appl. Polym. Symp.*, **33**, 3 (1978).
5. O. Ishizuka, K. Murase, K. Koyama, and K. Aoki, *Sen i Gakkaishi*, **31**(9), T-372 (1975).

6. H. I. Freeman and M. J. Coplan, *J. Appl. Polym. Sci.*, **8,** 2389 (1964).
7. S. Kase and T. Matsuo, *J. Appl. Polym. Sci.*, **11,** 251 (1967).
8. C. D. Han, R. R. Lamonte, and Y. T. Shah, *J. Appl. Polym. Sci.*, **16,** 3307 (1972).
9. S. Kase, *J. Appl. Polym. Sci.*, **18,** 3279 (1974).
10. C. B. Weinberger, G. F. Cruz-Saenz, and G. J. Donnelly, *AIChE J.*, **22,** 441 (1976).
11. H. Ishihara and S. Kase, *J. Appl. Polym. Sci.*, **20,** 167 (1976).
12. J. L. White and Y. Ide, *J. Appl. Polym. Sci.*, **22,** 3057 (1978).
13. T. Matsumoto and D. C. Bogue, *Polym. Eng. Sci.*, **18,** 564 (1978).
14. R. E. Christensen, *SPE J.*, **18,** 751 (1962).
15. A. Bergonzoni and A. J. D. Cresci, *Polym. Eng. Sci.*, **6,** 45, 50 (1966).
16. S. Kase, T. Matsuo, and Y. Yoshimoto, *Sen i Kikai Gakkaishi,* **19,** T63 (1966).
17. R. S. Spencer and R. E. Dillon, *J. Colloid Sci.*, **3,** 163 (1948).
18. A. B. Metzner, E. L. Carley, and I. K. Park, *Mod. Plast.* **37,** 133 (July 1960).
19. E. B. Bagley, S. H. Storey, and D. C. West, *J. Appl. Polym. Sci.*, **7,** 1661 (1963).
20. N. Nakajima and M. Shida, *Trans. Soc. Rheol.*, **10,** 229 (1966).
21. W. W. Graessley, S. D. Glasscock, and R. L. Crawley, *Trans. Soc. Rheol.*, **14,** 519 (1970).
22. R. A. Mendelson and F. L. Finger, *J. Appl. Polym. Sci.*, **12,** 797, (1973).
23. R. A. Mendelson and F. L. Finger, *J. Appl. Polym. Sci.*, **19,** 1061 (1975).
24. J. L. White and J. F. Roman, *J. Appl. Polym. Sci.*, **20,** 1005 (1976); **21,** 869 (1977).
25. C. D. Han and C. A. Villamizar, *J. Appl. Polym. Sci.*, **22,** 1677 (1978).
26. R. Racin and D. C. Bogue, *J. Rheol.*, **23,** 263 (1979).
27. D. Huang and J. L. White, *Polym. Eng. Sci.*, **19,** 609 (1979).
28. W. Minoshima, J. L. White, and J. E. Spruiell, *Polym. Eng. Sci.*, to appear.
29. J. E. Spruiell and J. L. White, *Polym. Eng. Sci.*, **15,** 660 (1975); *Appl. Polym. Symp.*, **27,** 121 (1975).
30. H. P. Nadella, H. M. Henson, J. E. Spruiell, and J. L. White, *J. Appl. Polym. Sci.*, **21,** 3003 (1977).
31. I. J. Chen, E. G. Hagler, L. E. Abbott, D. C. Bogue, and J. L. White, *Trans. Soc. Rheol.*, **16,** 473 (1972).
32. A. Ziabicki, *Fundamentals of Fiber Formation,* Wiley, London, 1976.
33. W. Thomson (Lord Kelvin) and P. G. Tait, *Treatise on Natural Philosophy,* Section 586, Cambridge University Press, 1879.
34. Y. Sano and K. Orii, *Sen i Gakkaishi,* **24,** 212 (1968).
35. G. V. Vinogradov, V. D. Fikham, and B. V. Radushkevich, *Rheol. Acta,* **11,** 286 (1972).
36. A. E. Everage and R. L. Ballman, *J. Appl. Polym. Sci.*, **20,** 1137 (1976).
37. Y. Ide and J. L. White, *J. Appl. Polym. Sci.*, **22,** 1061 (1978).
38. J. Meissner, *Rheol. Acta,* **8,** 78 (1969); *Trans. Soc. Rheol.*, **16,** 405 (1972).
39. F. N. Cogswell, *Appl. Polym. Symp.*, **27,** 1 (1975).
40. H. M. Laun and H. Munstedt, *Rheol. Acta,* **17,** 415 (1978).
41. A. Ziabicki and K. Kedzierska, *Kolloid Z.*, **52,** 51 (1959); **175,** 14 (1961).
42. S. Kase and T. Matsuo, *J. Polym. Sci., Part A,* **3,** 2541 (1965).
43. R. R. Lamonte and C. D. Han, *J. Appl. Polym. Sci.*, **16,** 3285 (1972).
44. M. Matsui and D. C. Bogue, *Polym. Eng. Sci.*, **16,** 735 (1976).
45. M. Matsui and D. C. Bogue, *Trans. Soc. Rheol.*, **21,** 133 (1977); T. Matsumoto and D. C. Bogue, *Trans. Soc. Rheol.*, **21,** 453 (1977).
46. M. M. Denn and G. Marrucci, *J. Non-Newt. Fluid Mech.*, **2,** 159 (1977).
47. C. J. S. Petrie, *J. Non-Newt. Fluid Mech.*, **4,** 137 (1978).
48. G. Zeichner, M.S. Thesis in Chemical Engineering, University of Delaware, 1973.
49. M. M. Denn, C. J. S. Petrie, and P. Avenas, *A.I.Ch.E. J.*, **21,** 791 (1975).
50. R. J. Fisher and M. M. Denn, *A.I.Ch.E. J.*, **22,** 237 (1976).
51. J. C. Chang and M. M. Denn, *J. Non-Newt. Fluid Mech.*, **5,** 369 (1979).
52. J. L. White and A. B. Metzner, *J. Appl. Polym. Sci.*, **8,** 1367 (1963).
53. Y. Ide and J. L. White, *J. Non-Newt. Fluid Mech.*, **2,** 281 (1977).
54. S. Middleman, *Fundamentals of Polymer Processing,* McGraw-Hill, New York, 1978.
55. A. B. Metzner, J. L. White, and M. M. Denn, *AIChE J.*, **12,** 863 (1966); *Chem. Eng. Prog.*, **62**(12), 81 (1966).
56. J. R. A. Pearson and M. A. Matovich, *Ind. Eng. Chem., Fundam.*, **8,** 605 (1969).
57. Y. T. Shah and J. R. A. Pearson, *Polym. Eng. Sci.*, **16,** 219 (1972).
58. Y. T. Shah and J. R. A. Pearson, *Ind. Eng. Chem., Fundam.*, **11,** 145, 150 (1972).
59. R. J. Fisher and M. M. Denn, *AIChE J.*, **23,** 23 (1977).

60. J. L. White, *J. Appl. Polym. Sci.*, **8,** 2339 (1964).
61. B. D. Coleman and H. Markovitz, *J. Appl. Phys.*, **35,** 1 (1969).
62. R. I. Tanner, *J. Polym. Sci., Part A-2,* **8,** 2067 (1970).
63. H. Janeschitz-Kriegl, *Adv. Polym. Sci.*, **6,** 170 (1969).
64. K. Oda, J. L. White, and E. S. Clark, *Polym. Eng. Sci.*, **18,** 53 (1978).
65. J. J. Hermans, P. H. Hermans, D. Vermaas, and A. Weidinger, *Rec. Trav. Chim.*, **65,** 427 (1946).
66. P. H. Hermans, J. J. Hermans, D. Vermaas, and A. Weidinger, *J. Polym. Sci.*, **3,** 1 (1948).
67. G. R. Taylor and S. R. Darin, *J. Appl. Phys.*, **26,** 1075 (1955).
68. R. S. Stein and F. H. Norris, *J. Polym. Sci.*, **21,** 381 (1956).
69. R. J. Samuels, *Structured Polymer Properties,* Wiley, New York, 1974.
70. R. J. Samuels, *J. Macromol. Sci., Phys.* **4,** 701 (1970).

Received May 11, 1979
Revised August 20, 1979